

## Article

# The Low Friction Coefficient and High Wear Resistance UHMWPE: The Effect of Pores on Properties of Artificial Joint Materials

Chunmin Yang<sup>1</sup>, Junhua Zhang<sup>2,\*</sup>, Honglin Yue<sup>3</sup> and Xueqin Kang<sup>4,\*</sup>

<sup>1</sup> School of Low-Carbon Energy and Power Engineering, China University of Mining and Technology, Xuzhou 221116, China; ychm\_cumt@163.com

<sup>2</sup> Xuzhou Technician Branch, Jiangsu Union Technical Institute, Xuzhou 221151, China

<sup>3</sup> Tianjin Zhongkuang New Materials Technology Limited Company, Tianjin 300350, China; honglin\_yhl@163.com

<sup>4</sup> School of Materials Science and Physics, China University of Mining and Technology, Xuzhou 221116, China

\* Correspondence: 13952186599@163.com (J.Z.); cumtkxq@cumt.edu.cn (X.K.)

**Abstract:** Ultrahigh-molecular-weight-polyethylene (UHMWPE) is extensively applied to make bone and cartilage implants in the field of biomaterial application. UHMWPE matched with a metal or ceramic component withstands the long-term effect of cyclic stress, which induces UHMWPE serious wear, and affects the service life of the artificial joint. This investigation focuses on the influence of pores on the mechanical and tribological property of UHMWPE. The porosity, crystallinity, yield strength, tensile strength, hardness, compression yield strength, creep resistance, wettability, friction performance, and wear mechanism of solid and porous UHMWPE were evaluated and compared. The research results indicated that the pore had a remarkable influence on the mechanical, friction, and wear property of UHMWPE. The porosity of porous UHMWPE was 29.7% when 50 wt. % sodium chloride (NaCl) was added and the pore size was about 200  $\mu\text{m}$ . The crystallinity, hardness, creep resistance, strength, and elongation decreased after NaCl was added and dissolved. However, the yield strength in the tensile and compression test was closer to that of the natural cartilage. The friction coefficient and wear loss of porous UHMWPE were higher than that of solid UHMWPE in dry conditions, but these values of porous UHMWPE were lower than that of solid UHMWPE in the calf serum lubrication condition. The main wear mechanism of porous and solid UHMWPE was abrasive. The lubricity of calf serum reduced wear surface scratches and furrows, especially for porous UHMWPE.

**Keywords:** polymers; FTIR; squeeze-film lubrication; viscoelasticity; abrasive wear



Received: 25 November 2024

Revised: 7 January 2025

Accepted: 8 January 2025

Published: 13 January 2025

**Citation:** Yang, C.; Zhang, J.; Yue, H.; Kang, X. The Low Friction Coefficient and High Wear Resistance UHMWPE: The Effect of Pores on Properties of Artificial Joint Materials. *Lubricants* **2025**, *13*, 31. <https://doi.org/10.3390/lubricants13010031>

**Copyright:** © 2025 by the authors. Licensee MDPI, Basel, Switzerland. This article is an open access article distributed under the terms and conditions of the Creative Commons Attribution (CC BY) license (<https://creativecommons.org/licenses/by/4.0/>).

## 1. Introduction

Ultrahigh-molecular-weight-polyethylene (UHMWPE) is extensively serviced for bone and cartilage implants due to its self-lubricating property, wear resistance, bioavailability, and chemical stability [1–3]. The durability and wear of UHMWPE are the main problems with UHMWPE-on-ceramic (or metal) artificial implants, particularly used as artificial cartilage in total joint replacement [1,4]. Articular cartilage is composed of many biological macromolecules, for instance, aggrecan, lubricant, hyaluronan, and phosphatidylcholine liposomes. The amphoteric head groups of the phosphatidylcholine liposomes absorb water to create a tough hydration film around the charges, resulting in a significant decrease in the friction coefficient between joints, usually as little as 0.001–0.01 [5–8]. UHMWPE is used to produce porous implants as close to articular cartilage as possible. Traditional foaming

methods, such as gas foaming, phase separation, and sintering cannot be used because the molecular weight of UHMWPE is very high [9]. The foaming agent used in porous UHMWPE as a material for bone or cartilage implants should be non-toxic. Sodium chloride (NaCl), as a component of human body fluids, can maintain the normal morphology of cells. NaCl can be served as a pore-forming filler to produce porous materials, and the porosity of these materials can reach 60–70% [9,10].

Wu et al. prepared porous UHMWPE with different porosity by the NaCl template leaching method. They found that the friction and wear property were improved by pores under water lubrication, but the pore structure and other mechanical performance of this material were not mentioned [11]. Chou et al. adopted the same approach to study the porosity distribution and tribological behavior of porous UHMWPE. In physiological saline, the abrasion performance of porous UHMWPE was inferior to solid UHMWPE, and the percentage of abrasive chips in the reaction size range of the foreign body was smaller, but wettability and mechanical properties of porous UHMWPE, such as the tensile test, compression performance, hardness, and creep resistance, were not involved [12]. Maksimkin et al. fabricated multilayer porous UHMWPE scaffolds to mimic the structure of trabecular and maintain its adaptability, but this material only applied to trabecular bone and was free from the force of torsion, bending, compression, and friction [9]. Sun et al. manufactured UHMWPE foams by the one-step batch foaming method, but this material was mainly used for heat insulation and the separation of oil and water [13]. Wang et al. reported UHMWPE/PEG porous materials with both large and small cells and demonstrated the evolution of micropore morphology and mechanical properties, but mainly focused on the compression performance [14]. Li et al. fabricated porous UHMWPE/PVDF/MWCNT used PLA and PMMA as a sacrificial template and tested the electromagnetic shielding performance [15]. Azam et al. manufactured cellular structures GNP/UHMWPE via selective laser sintering and tested the mechanical and piezoresistive properties [16]. Zhu et al. prepared oil-containing modified porous UHMWPE composites and tested frictional performance under pure and seawater conditions [17]. Salimon et al. also obtained porous UHMWPE through the sacrificial template method and tested compression and tensile and bending properties with different pore sizes [10]. Wettability, hardness, and friction and wear properties were equally important in the performance of cartilage materials as strength.

In this work, solid and porous UHMWPE specimens were fabricated by thermal compression molding. NaCl particles were used as space-holder material to increase the porosity and were removed sufficiently by water leaching after sintering. The effect of NaCl on density, porosity, and pore structure was investigated. The tensile test, compression test, hardness, creep resistance, and especially the tribological performance of porous UHMWPE were measured and analyzed.

## 2. Experiment

### 2.1. Materials and Fabrication Methods

Medical UHMWPE (GUR 4150, provided by Shanghai Hualan Chemical Technology Limited Company, Shanghai, China), with a molecular mass of 9 million and a density of  $930 \text{ kg/m}^3$ , is in powder form. NaCl particles with a pure degree of 99.8% and a density of  $2170 \text{ kg/m}^3$  were purchased from Aladdin.

The UHMWPE and NaCl powders were mingled in an agitator for 15 min. The content of NaCl particles was 50 wt.% according to a study reported by Wu [11] because the continuity of the UHMWPE matrix and the connectivity of the pores were ensured. The powder mixtures were added into a mold and hot-pressed on a flat vulcanizing machine. The pressure, temperature, and time were set as 15 MPa,  $200 \text{ }^\circ\text{C}$ , and 2 h, respectively.

The final products with different dimensions were cooled with the equipment to normal temperature. The NaCl particles were removed from the sintered products by water leaching at a temperature of 40 °C for two weeks and the water once a day for purification. The porous UHMWPE specimens were placed into a dryer at 50 °C for 8 h to eliminate dampness. The masses of the porous UHMWPE were measured before and after leaching to calculate the dissolution ratio of NaCl and the porosity of UHMWPE.

### 2.2. Pore and Porosity Characterization

The scanning electron microscopy (SEM) images of pore structure were captured by FEI Quanta TM 250 under the condition of high vacuum and 20 kV accelerating voltage.

The porosity of porous UHMWPE was counted through Equation (1).

$$\theta = \frac{W_L}{\frac{\rho_1}{\rho_2} + 1} \times 100\% \quad (1)$$

where  $\theta$  is the porosity value of porous UHMWPE,  $W_L$  is the dissolution rate of NaCl in porous UHMWPE,  $\rho_1$  is the density of NaCl, and  $\rho_2$  is the density of UHMWPE.

The dissolution rate of NaCl in porous UHMWPE was calculated through Equation (2).

$$W_L = \frac{W_1 - W_2}{W_1} \times 100\% \quad (2)$$

where  $W_1$  is the mass of the UHMWPE specimen before NaCl dissolution, and  $W_2$  is the mass of UHMWPE specimen after NaCl dissolution.

### 2.3. Fourier Transform Infrared and Differential Scanning Calorimetry

The effect of the molding process on the molecular structure was investigated through Fourier transform infrared (FTIR) on Vertex 80v. The measurement was performed from 500 to 4000  $\text{cm}^{-1}$ , with a scan resolution of 4  $\text{cm}^{-1}$ . Differential scanning calorimetry (DSC) was used to measure and estimate the crystallinity. A sample (~20 mg) was heated from 30 to 200 °C and held at 200 °C for 5 min. The sample was cooled to 30 °C and then heated to 200 °C again. The rate of heating and cooling was 10 °C/min. The crystallinity of solid and porous UHMWPE was counted through Equation (3). The results of three samples for each type of UHMWPE were averaged.

$$\chi_c = \frac{\Delta H}{\Delta H_{100}} \times 100\% \quad (3)$$

where  $\Delta H$  is the integrated enthalpy of fusion, which was obtained by integrating the area under endothermic peak between 80 and 160 °C, and  $\Delta H_{100}$  is the enthalpy of fusion for 100% crystalline polyethylene, which is considered 289.3 J/g [4,18].

### 2.4. Wettability Testing

The apparatus (JCB2000B, Beijing Zhongyi Kexin Technology Limited Company, Beijing, China) was employed to measure the contact angle. A syringe was skillfully used to drop calf serum on the solid and porous UHMWPE surface, then we captured the image and measured the contact angle within 30–120 s after the calf serum dropped onto the specimen surface. Each specimen was tested ten times and then averaged. UHMWPE wettability and the hydrophilicity/hydrophobicity ratio of the material surface was reflected by the measured contact angle [3].

### 2.5. Mechanical Performance Characterization

The tensile specimen was performed on a tensile test machine in accordance with ISO 527 [19], with a stretch speed of 50 mm/min. During the test, the stress–strain curve was recorded automatically after the specimen dimension input. The specimen used in this experiment was manufactured according to Reference [4]. The results of three samples for each type of UHMWPE were averaged.

The stress on anti-abrasive material was usually compressive strength. The specimen dimension of solid and porous UHMWPE was  $(10 \times 10 \times 5) \text{ mm}^3$ . The compression test was carried out on a WDW-5 according to the standard ISO 604 [20]. The specimen of the solid and porous UHMWPE was compressed to 250 N and then unloaded the force to zero. The force and deformation curves were recorded to check the stress and deformation recovery capacity during the loading and unloading process, respectively. The results of five samples for each type of UHMWPE were averaged.

To research the effect of pores on the hardness of UHMWPE, shore hardness (SH) was used according to the standard ISO 868 and calculated automatically [21]. Each sample was tested ten times and then averaged.

The polymer continued to produce creep deformation under the constant external force. Serious deformation caused by creep influenced the precision of implant and led to its failure [22]. Creep behaviors of solid and porous UHMWPE were characterized through a ball indentation creep experiment. Each sample was tested five times and then averaged.

### 2.6. Friction Experiment

A tribological property experiment was performed on a tribo-testing machine to assess the friction and wear performance of solid and porous UHMWPE. Experimental heating, insulation, lubrication, and methods were described in detail in Reference [4]. The test load, temperature, sliding speed, and reciprocating distance were 19.8 N,  $37 \pm 1 \text{ }^\circ\text{C}$ , 2 mm/s, and 10 mm, respectively. This test load resulted in a central contact pressure of 85.2 MPa between the ball and the porous UHMWPE specimen, corresponding to the central contact pressure for a ceramic ball with a diameter of 28 mm on the UHMWPE cup applied by the peak load of the body weight of 75 kg [23]. Calf serum solution (25 vol. %) and deionized water were used as lubricants, and the whole test lasted for 7200 s. The friction coefficient recorded during the test and wear mass loss were taken as the wear parameters to estimate the friction performance of solid and porous UHMWPE. Each sample was tested five times and then averaged. The wear mechanism was also analyzed by SEM.

## 3. Results and Discussion

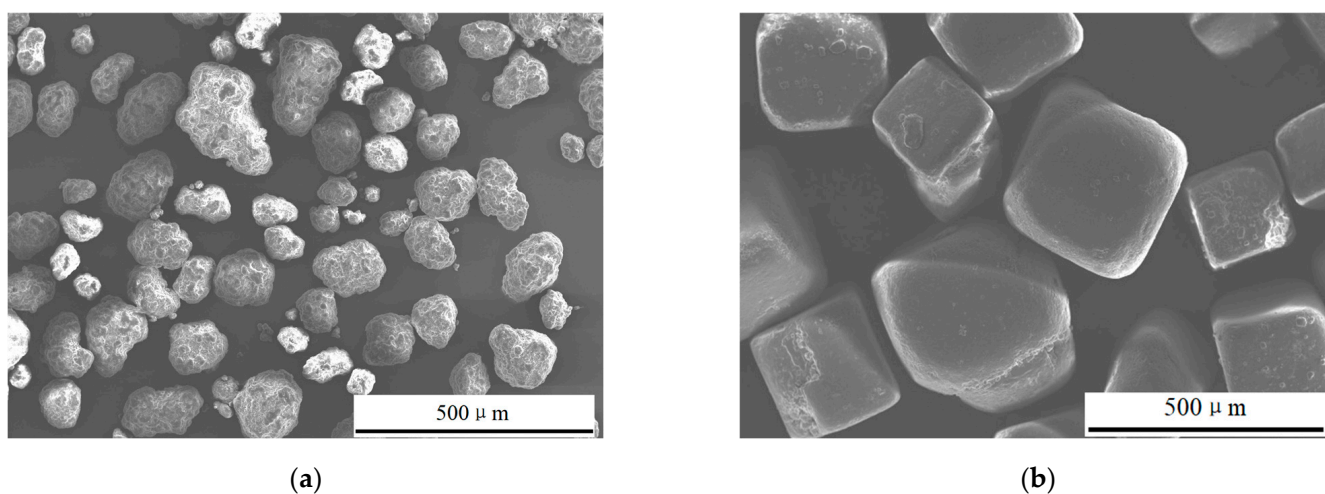
### 3.1. SEM Analysis of NaCl and UHMWPE

Figure 1 presents the morphology of UHMWPE and NaCl. The mean particle size of UHMWPE was 88.64  $\mu\text{m}$ , distributing between 21.12~179.75  $\mu\text{m}$ . UHMWPE powder had an irregular particle structure with protuberances on its surface. The NaCl particle was a regular cube, and the average size was about 200  $\mu\text{m}$ . In natural cartilage, the pore sizes are mainly concentrated in the range of 0.01~0.03, 7~15, and 30~150  $\mu\text{m}$  [24]. NaCl with a particle size close to 30~150  $\mu\text{m}$  was used as a template to fabricate porous materials.

The weights of UHMWPE samples before and after NaCl dissolution were  $19.41 \pm 0.28$ , and  $9.52 \pm 0.06$  g, respectively. The dissolution rate of NaCl reached 49%, indicating that a very small amount of NaCl was encapsulated by UHMWPE in the matrix. The volume porosity of porous UHMWPE was 29.7%, based on the dissolution rate of NaCl and the density of NaCl and UHMWPE. Figure 2 shows the micrographs of solid and porous UHMWPE. The pores of porous UHMWPE replicated from NaCl were opened and interconnected. The hole size ranged from tens to hundreds of microns, and the size of the



largest hole was 200  $\mu\text{m}$ , corresponding to the added NaCl particle size. The shape of the pore is inherited from the space holder, and the porosity is related to the amount of space holder added, both of which have an impact on the performance of porous UHMWPE.



**Figure 1.** SEM images of (a) UHMWPE and (b) NaCl particles.

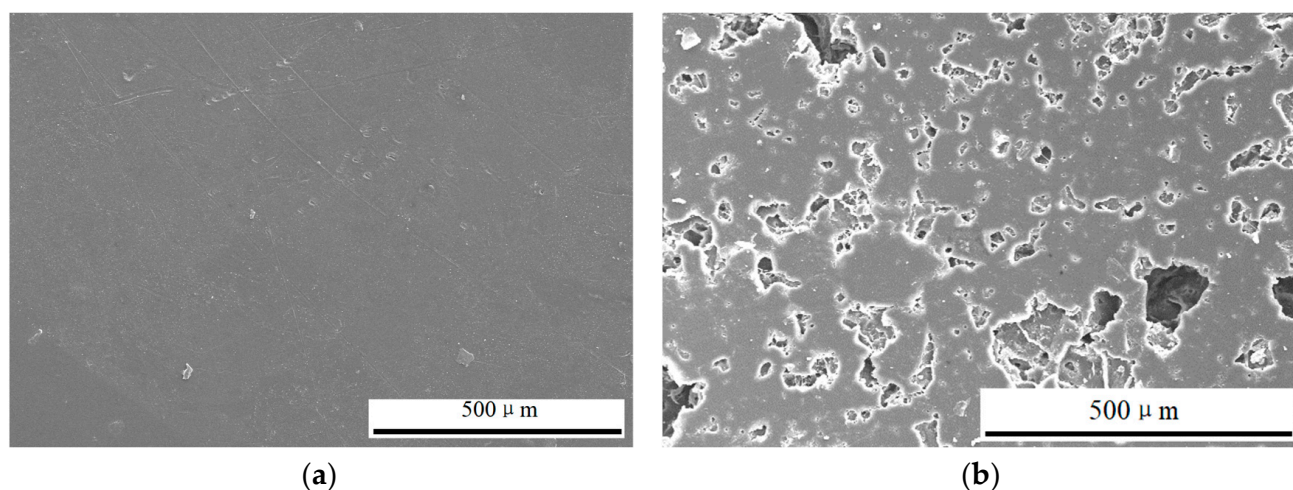


**Figure 2.** SEM images of (a) solid and (b) porous UHMWPE.

### 3.2. FTIR Analysis

FTIR spectra of UHMWPE powder and sintered (solid or porous) UHMWPE are shown in Figure 3. The peaks from 680 to 780  $\text{cm}^{-1}$  and 1430 to 1470  $\text{cm}^{-1}$  represented the rocking and bending deformation of polyethylene [25]. The peaks around 2835 and 2910  $\text{cm}^{-1}$  represented the asymmetrical and symmetrical stretching of  $\text{CH}_3\text{-CH}_2\text{-}$  and  $\text{-CH}_2\text{-CH}_2\text{-}$  groups, respectively [25]. The peaks from 1650 to 1850  $\text{cm}^{-1}$  corresponded to the absorption of carbonyl species and 1100 to 1400  $\text{cm}^{-1}$  associated with  $\text{-C-O-C-}$  vibrations [26]. These indicated that the UHMWPE was oxidized during the molding process. Mechanical properties of UHMWPE were weakened owing to the oxidation [27], so antioxidants such as Vitamin E [8,28], butylated hydroxytoluene [29], butyl hydroxy anisole [30] and natural polyphenols [31] were used to prevent UHMWPE oxidation.

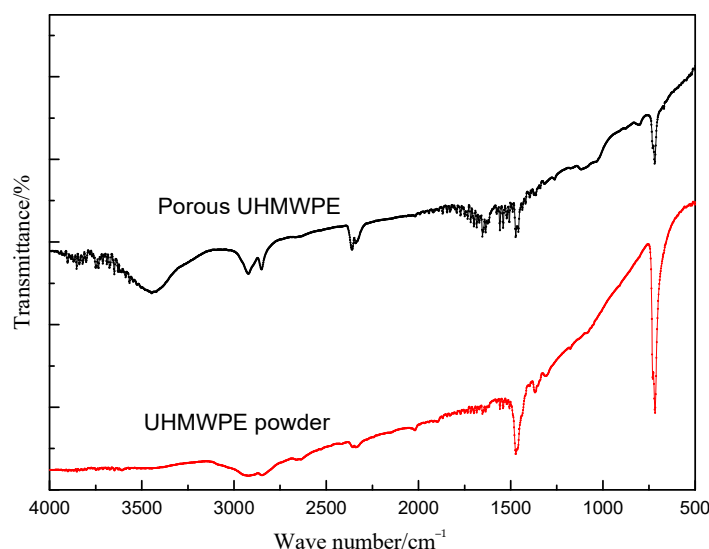


**Figure 3.** FTIR spectra of UHMWPE powder and porous UHMWPE.

### 3.3. Crystallinity Analysis

The crystallinity values of solid and porous UHMWPE were  $50.0 \pm 0.5$  and  $48.7 \pm 0.5\%$ , respectively. The crystallinity of porous UHMWPE decreased due to the addition of NaCl. The thermal capacity of NaCl ( $0.88 \text{ kJ/kg } ^\circ\text{C}$ ) was lower than that of UHMWPE ( $1.84 \text{ kJ/kg } ^\circ\text{C}$ ). This shows that the heat absorbed by NaCl was less than that of UHMWPE in the molding process when the same temperature was raised. The heat absorption of UHMWPE was insufficient due to the manufacturing system being commanded by temperature. Also, the compression effect of external force on the UHMWPE matrix was reduced because NaCl particles undertook part of the force [12]. UHMWPE, as a semi crystalline material, contains the phases of crystalline and amorphous [4,7]. The insufficient heat and actuated pressure reduced the mobility of UHMWPE chains, and this formed less crystalline lamellae in the molding process, resulting in the crystallinity of porous UHMWPE reduction.

### 3.4. Wettability Analysis

The friction property of materials is related to the contact angle or wettability under lubrication [32]. Materials with a larger contact angle were prone to forming and maintaining a lubricating film due to the lower diffusion ability of lubricants on the sample surface. In this case, the coefficient of friction is reduced, and the wear resistance is enhanced [33]. Meanwhile, the specimen with a small contact angle permits the lubricant to extend on its surface, and the lubricating film cannot be formed and kept, resulting in a high friction coefficient and low wear resistance.

Figure 4 presents a micrograph of the contact angle between UHMWPE and deionized water. The contact angle values of solid UHMWPE with deionized water and calf serum were  $85 \pm 3$  and  $81 \pm 3^\circ$ , and these values of porous UHMWPE were  $54 \pm 2$  and  $58 \pm 2^\circ$ , respectively. The change in the solid material surface microstructure led to the change in the intrinsic contact area and contact angle. Yin et al. considered that, due to the existence of a coarse surface, the real contact area between the liquid and the solid material was larger than the apparent contact area, thus improving the hydrophilicity [34]. The fluid was easily inhaled into the pores, which transformed the surface and interface performance, resulting in the decrease in the contact angle [35]. The macromolecular proteins in calf serum rubbed with the pore wall when they penetrated the pores, which prevented calf serum from continuing to penetrate. Therefore, the change in contact angle with calf serum from solid to porous UHMWPE was less than that with deionized water.

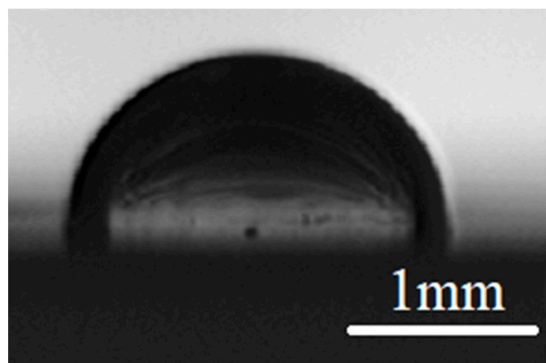


**Figure 4.** Microscopic picture of the contact angle between UHMWPE and deionized water.

### 3.5. Hardness Test Analysis

The SH value of solid UHMWPE was  $67.9 \pm 1.3$  HD, and these values of porous UHMWPE were  $69.5 \pm 3.4$  and  $48.9 \pm 2.1$  HD before and after the dissolution of NaCl, respectively. The hard NaCl particles hindered the deformation of the soft UHMWPE matrix and then led to an increase in the hardness [36]. But the addition of NaCl reduced the crystallinity and then reduced the hardness of UHMWPE. Pores were formed in situ after the dissolution of NaCl. The hardness of porous UHMWPE decreased obviously due to the pores' weakening action and crystallinity decrease [37].

### 3.6. Tensile Test Analysis

The tensile stress–strain of solid and porous UHMWPE have the same profiles, respectively. Figure 5 demonstrates the typical tensile stress–strain profiles of solid and porous UHMWPE. The tensile curves included two different stages. In the first stage, only elastic deformation occurred; the length of the specimen increased in proportion to the stress increase. The dimension of the sample returned to its incipient size; when applied, stress was expunged. In the second stage, plastic deformation strengthening appeared, and the dimension could not restore when the applied stress was removed. The sample was pulled apart, and the stress decreased sharply when the stress exceeded the strength of UHMWPE. The yield strengths of solid and porous UHMWPE were  $21.0 \pm 1.7$  and  $8.4 \pm 0.5$  MPa, while the tensile strengths were  $29.5 \pm 1.6$  and  $12.4 \pm 0.7$  MPa, respectively. The elongation of porous UHMWPE was  $27.4 \pm 0.5\%$ . The elongation of solid UHMWPE was larger than that of porous UHMWPE, but the detailed extensibility value of solid UHMWPE could not be measured due to the sample curling after a fracture. Although the yield strength of solid UHMWPE was higher than that of porous UHMWPE, the yield strength of porous UHMWPE was closer to that of natural cartilage ( $\sim 5.80$  MPa) [38].

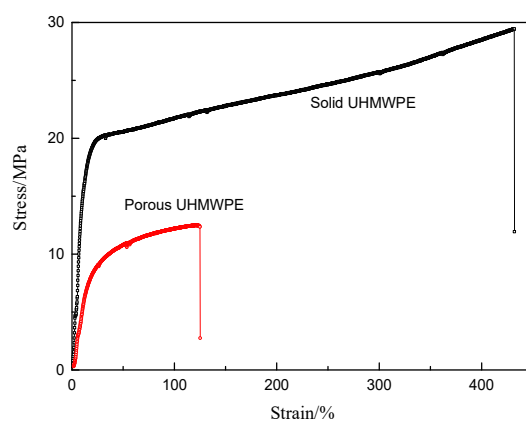


**Figure 5.** Typical tensile stress–strain profiles of solid and porous UHMWPE.

### 3.7. Compression and Recovery Test Analysis

The compression and recovery performance of solid and porous UHMWPE have the same trend of change, respectively. Figure 6 shows the typical resistance and deformation recovery curves of solid and porous UHMWPE to force in dry conditions and calf serum. The change in force applied on the solid UHMWPE was very sharp under the small deformation, while the porous UHMWPE had a large deformation under the same load, and there was a buffering effect on the force applied to the material. This buffering effect was caused by the liquid-holding capacity of porous materials. The compressive yield strength of solid UHMWPE was  $25.9 \pm 0.7$  MPa, whether in dry conditions or calf serum. The compressive yield strengths of porous UHMWPE in dry conditions and calf serum were  $7.0 \pm 0.3$  and  $7.3 \pm 0.4$  MPa, respectively. The strength of porous UHMWPE had little change in dry conditions and calf serum and was closer to that of natural cartilage ( $\sim 3.7$  MPa) [39].

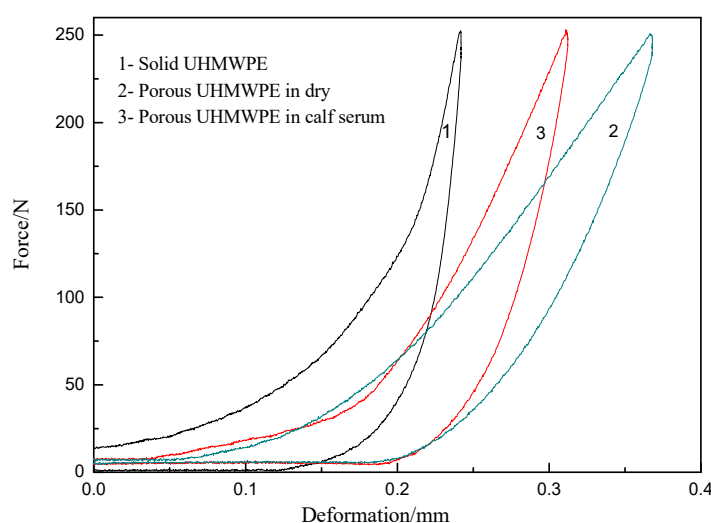


**Figure 6.** Typical force and deformation curves of solid and porous UHMWPE in the loading and unloading process.

### 3.8. Creep Resistance Analysis

The typical indentation depth changes in solid and porous UHMWPE with time are shown in Figure 7. In the ball compression creep test, the indentation depth increased significantly at the beginning of 500 s, and, then, the increase slowed down. The final indentation depth of solid UHMWPE was  $0.102 \pm 0.008$  mm, whether in dry conditions, deionized water, or calf serum. The final indentation depths of porous UHMWPE in dry conditions, deionized water, and calf serum sample were  $0.271 \pm 0.016$ ,  $0.264 \pm 0.013$ , and  $0.254 \pm 0.012$  mm, respectively. The reasons for the change in indentation depth are as follows: First, the weakening effect of the pore makes the porous UHMWPE produce more deformation. Second, the pores in porous UHMWPE promote the motion ability of the UHMWPE molecules and reduce the creep resistance. Therefore, the indentation depth of porous UHMWPE, whether in dry conditions, deionized water, or calf serum, is larger than that of solid UHMWPE. The final indentation depth reduced about 0.007 and 0.017 mm due to the presence of deionized water and calf serum, which indicated that the creep resistance of porous UHMWPE was enhanced, and porous UHMWPE still had a certain liquid-holding capacity under long-term pressure.



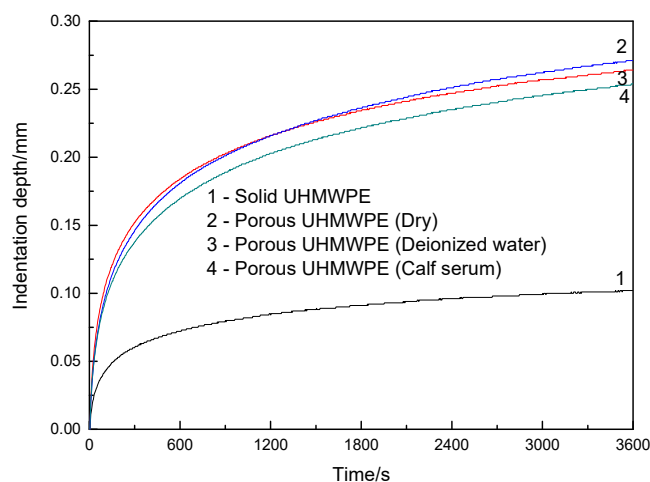


**Figure 7.** The change in indentation depth of solid and porous UHMWPE with time under different mediums.

### 3.9. Friction Property and Wear Mechanism

The coefficient of friction and wear amount were usually utilized to reveal friction and wear property of materials. Figure 8 exhibits the typical friction coefficient of solid and porous UHMWPE in dry conditions, deionized water, and calf serum. To all samples, the initial friction coefficient values changed greatly and then reached equilibrium. The stable friction coefficient values of solid and porous UHMWPE in dry conditions were  $0.185 \pm 0.005$  and  $0.278 \pm 0.012$ , and these values decreased to  $0.102 \pm 0.003$  and  $0.075 \pm 0.002$ ,  $0.038 \pm 0.001$  and  $0.020 \pm 0.001$  in deionized water and calf serum, respectively. The surface roughness and real stress on porous UHMWPE increased due to the existence of pores, and the friction force increased, which led to a significant increase in the friction coefficient in dry conditions. Figure 9 displays the lubrication model of porous material. The liquid in the pores bore part of the pressure due to the liquid-holding capacity of the pore, resulting in a decrease in real stress on UHMWPE and a reduction in frictional force. Porous UHMWPE showed a low friction coefficient under the action of liquid lubrication. The friction coefficient was not only related to the liquid lubricity but also to the pore-holding capacity caused by the viscosity of the liquid and pore. Therefore, the friction coefficient values of solid or porous UHMWPE in deionized water and calf serum were lower than that in dry conditions. Compared with solid UHMWPE, porous UHMWPE had better liquid-holding ability, and its friction coefficient value was lower than that of solid UHMWPE. The friction coefficient of porous UHMWPE in dry conditions was higher than that of solid UHMWPE because the pore reduced the real stress area and then increased the real stress. The friction coefficient values of solid and porous UHMWPE in dry conditions ( $0.185$  and  $0.278$ ) were almost the same as that of dry cartilage ( $0.25$ ) [40]. The friction coefficient of porous in calf serum ( $0.020$ ) was lower than that of solid UHMWPE ( $0.038$ ), but it was still higher than that of natural cartilage in the synovium ( $0.005$ ) [40]. The wear loss values of solid and porous UHMWPE in dry conditions were  $0.25 \pm 0.02$  and  $1.13 \pm 0.05$  mg, and these values changed to  $0.19 \pm 0.02$  and  $0.09 \pm 0.01$  mg in calf serum, respectively. The wear resistance of porous UHMWPE was lower than that of solid UHMWPE in dry conditions because the continuity of porous UHMWPE was damaged by the pore. Calf serum stored in porous UHMWPE was released to the surface and acted as a lubricant during the process of friction and wear. Due to the lubricating effect of calf serum, the wear resistance of solid UHMWPE in calf serum was superior to that in dry conditions. Meanwhile, the wear resistance of porous UHMWPE was superior to that of solid UHMWPE in calf serum because the formed lubricating film on the solid UHMWPE surface was easy to destroy.

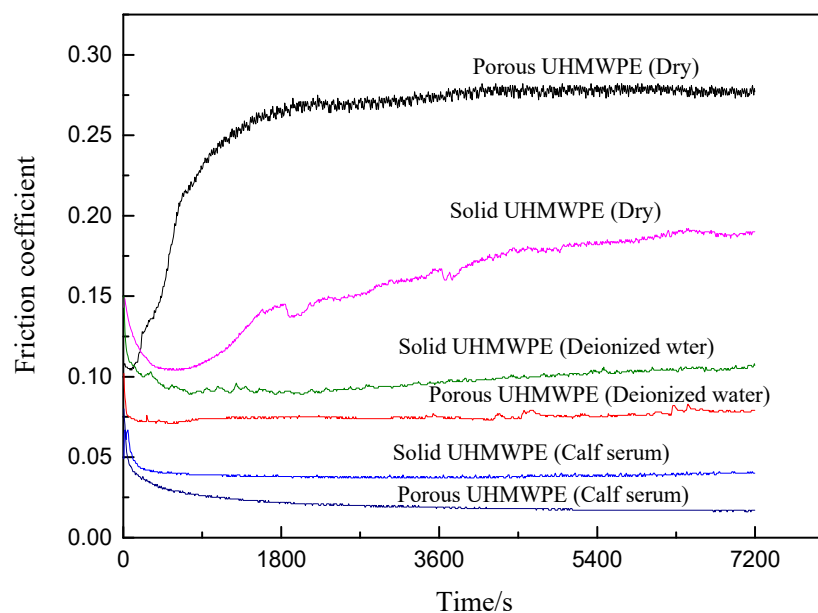


**Figure 8.** Typical friction coefficient profiles of solid and porous UHMWPE in different mediums.

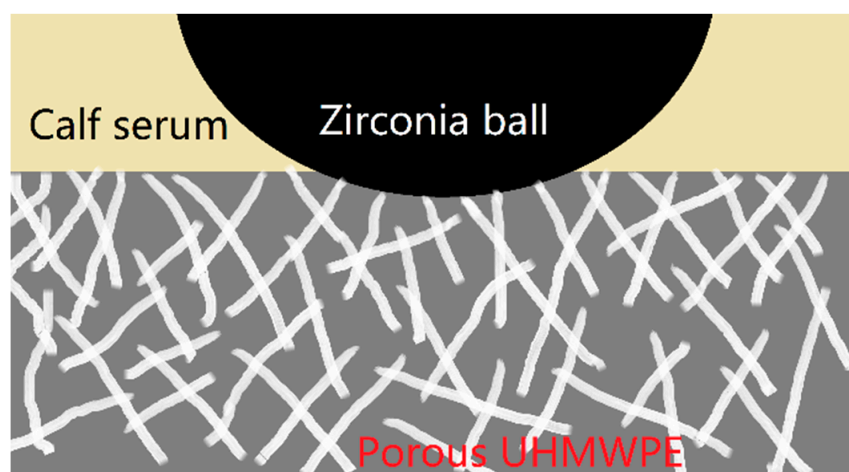


**Figure 9.** Lubrication model of porous UHMWPE.

Figure 10 displays SEM images of abrasion marks on a solid and porous UHMWPE surface. The worn surface was distributed with slight scratches and shallow furrows along the friction direction; these were the main characteristic of abrasive wear. The heat was generated by the friction between UHMWPE and the ceramic ball and caused the thermal softening of UHMWPE, resulting in scratches and furrows on wear marks [36]. There were some folds on the grinding marks of porous UHMWPE because the continuity of UHMWPE was destroyed by the pores. The wear mass loss of porous UHMWPE in dry conditions was the largest in all UHMWPE samples. The scratches and furrows on the solid and porous UHMWPE surface in calf serum were very light, especially on the porous UHMWPE. There were almost no scratches or furrows. Therefore, the wear loss of porous UHMWPE in calf serum was the least in all UHMWPE samples.

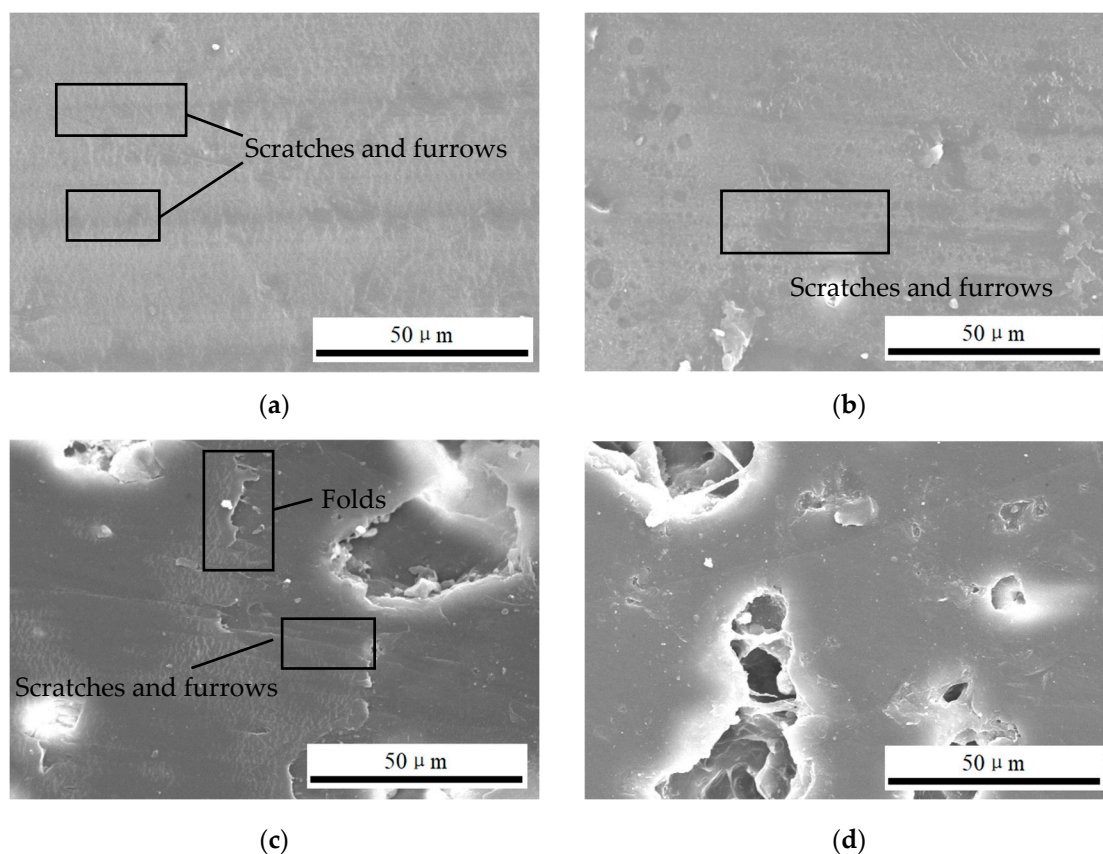


**Figure 10.** SEM images of abrasion marks on (a) solid and (c) porous UHMWPE under dry friction, and (b) solid and (d) porous under calf serum lubrication.

#### 4. Conclusions

UHMWPE and NaCl/UHMWPE samples were produced by the compression molding method. Then, the NaCl in UHMWPE was completely dissolved, and the pores formed in situ of dissolved NaCl. The porosity of the porous UHMWPE was 29.7% when the addition of NaCl was 50 wt. % and the average pore size was 200 μm. The crystallinity of UHMWPE decreased due to the addition of NaCl. Mechanical properties such as hardness, creep resistance, strength, and elongation were decreased due to the weakening effect of the pore and crystallinity decrease. However, the yield strength of porous UHMWPE was closer to that of the natural cartilage in the tensile and compression test. At the same time, the porous UHMWPE had a better buffering effect on the force due to the pore's liquid-holding capacity. To both solid and porous UHMWPE, the friction coefficient was lower, and the wear resistance was higher in calf serum than that in dry conditions because calf serum played a lubricating role during friction and wear test. In dry conditions, porous UHMWPE had a higher friction coefficient and lower wear resistance than that of solid UHMWPE due to the continuity of UHMWPE, which was damaged, and the real stress applied on the UHMWPE was increased. Meanwhile, in calf serum, porous UHMWPE had a lower friction coefficient and wear resistance than that of solid UHMWPE because the liquid in the pores bore part of the pressure and overflowed under the action of pressure, forming a complete lubrication film. The wear mechanism of solid and porous UHMWPE was abrasive wear. The scratches and furrows on grinding marks were reduced by the lubricity of calf serum, especially in porous UHMWPE.

In future work, the content of space holder material can be changed to alter the porosity of porous UHMPWE, making it closer to the performance of cartilage. The shape and particle size of the space holder can also be changed to study their effect on the properties of

porous UHMWPE. When the performance of porous UHMWPE is comparable to cartilage, its rheological behavior and dynamic mechanical analysis should be studied.

**Author Contributions:** Methodology, C.Y., H.Y. and J.Z.; validation, C.Y. and X.K.; formal analysis, J.Z.; investigation, C.Y., H.Y. and X.K.; writing—original draft, C.Y., J.Z. and X.K.; visualization, H.Y.; supervision, C.Y. and X.K.; project administration, X.K. All authors have read and agreed to the published version of the manuscript.

**Funding:** This work was supported by the Fundamental Research Funds for the Central Universities (grant number 2019XKQYMS17).

**Data Availability Statement:** The original contributions presented in this study are included in the article; further inquiries can be directed to the corresponding authors.

**Conflicts of Interest:** Author Honglin Yue was employed by Tianjin Zhongkuang New Materials Technology Limited Company. The remaining authors declare that the research was conducted in the absence of any commercial or financial relationships that could be construed as a potential conflict of interest.

## References

1. Kurtz, S.M. *UHMWPE Biomaterials Handbook: Ultra-High Molecular Weight Polyethylene in Total Joint Replacement and Medical Devices*, 3rd ed.; Elsevier: Oxford, UK, 2016.
2. Lan, J.; Mo, C.; Chen, X.; Hu, T.; Li, X.; Zhang, C. Carbon fiber/nano SiO<sub>2</sub> reinforced polyelectrolyte-graft UHMWPE for water lubricated superlubricity. *Tribol. Int.* **2025**, *202*, 110303. [[CrossRef](#)]
3. Duraccio, D.; Strongone, V.; Malucelli, G.; Auriemma, F.; De Rosa, C.; Mussano, F.D.; Genova, T.; Faga, M.G. The role of alumina-zirconia loading on the mechanical and tribological properties of UHMWPE for biomedical application. *Compos. Part B Eng.* **2019**, *164*, 800–808. [[CrossRef](#)]
4. Kang, X.; Zong, X.; Zhang, P.; Zeng, X.; Liu, Y.; Yao, C.; Wang, T.; Feng, P.; Yang, C. Effects of epigallocatechin gallate incorporation in UHMWPE on biological behavior, oxidative degradation, mechanical and tribological performance for biomedical applications. *Tribol. Int.* **2021**, *15*, 106887. [[CrossRef](#)]
5. Li, A.; Su, F.; Chu, P.K.; Sun, J. Articular cartilage inspired bilayer coating on Ti6Al4V alloy with low friction and high load-bearing properties. *Appl. Surf. Sci.* **2020**, *515*, 146065. [[CrossRef](#)]
6. Jahn, S.; Klein, J. Lubrication of articular cartilage. *Phys. Today* **2018**, *71*, 48–54. [[CrossRef](#)]
7. Chen, H.; Sun, T.; Yan, Y.; Ji, X.; Sun, Y.; Zhao, X.; Qi, J.; Cui, W.; Deng, L.; Zhang, H. Cartilage matrix-inspired biomimetic superlubricated nanospheres for treatment of osteoarthritis. *Biomaterials* **2020**, *242*, 119931. [[CrossRef](#)] [[PubMed](#)]
8. Yang, C.; Zhang, P.; Wang, T.; Kang, X. The role of simulated body fluid and force on the mechanical and tribological properties of  $\alpha$ -tocopherol stabilized UHMWPE for biomedical applications. *Polym. Bull.* **2021**, *78*, 6517–6533. [[CrossRef](#)]
9. Maksimkin, A.V.; Senatov, F.S.; Anisimova, N.Y.; Kiselevskiy, M.V.; Zalepugin, D.Y.; Chernyshova, I.V.; Tilkunova, N.A.; Kaloshkin, S.D. Multilayer porous UHMWPE scaffolds for bone defects replacement. *Mater. Sci. Eng. C* **2017**, *73*, 366–372. [[CrossRef](#)] [[PubMed](#)]
10. Salimon, A.I.; Statnik, E.S.; Zadorozhnyy, M.Y.; Senatov, F.S.; Zherebtsov, D.D.; Safonov, A.A.; Korsunsk, A.M. Porous open-cell UHMWPE: Experimental study of structure and mechanical properties. *Materials* **2019**, *12*, 2195. [[CrossRef](#)] [[PubMed](#)]
11. Wu, G.; Zhao, C.; Qin, H.; Zhao, X. Preparation and tribological behaviors of porous UHMWPE using as artificial cartilage. *Adv. Mater. Res.* **2011**, *199–200*, 651–654. [[CrossRef](#)]
12. Chou, C.C.; Wang, Y.Z.; You, J.H.; Wu, C.L. Tribological and oxidative properties of porous high-pressure crystallized and vitamin E-incorporated ultra-high-molecular weight polyethylene as an artificial cartilage. *Adv. Mech. Eng.* **2015**, *7*, 1–7. [[CrossRef](#)]
13. Sun, X.; Wang, G.; Xu, Z.; Chai, J.; Zhang, A.; Zhao, G.; Li, S.; Wang, Y.; Jiao, H. Microcellular foaming-derived strong ultra-high molecular weight polyethylene/high-density polyethylene foams for thermally insulating and oil-water separating applications. *J. Environ. Chem. Eng.* **2024**, *12*, 113992. [[CrossRef](#)]
14. Wang, L.; Cui, P.; Bi, Z.; Wang, C.; Zhou, B.; Zheng, L.; Niu, H.; Sun, X.; Wang, J.; Wang, D.; et al. Microcell morphology evolution and mechanical performance of UHMWPE/PEG porous materials with bimodal cell structure. *Compos. Struct.* **2023**, *322*, 117347. [[CrossRef](#)]
15. Li, Y.; Song, D.; Chen, Q.; Liu, Y.; Zheng, Y.; Nie, C.; Jia, Y.; Zheng, H.; Wei, F. Polymer blend templated hierarchical porous composites with segregated structure and enhanced electromagnetic interference shielding performance. *Polym. Compos.* **2023**, *44*, 9087–9100. [[CrossRef](#)]

16. Azam, M.U.; Schiffer, A.; Kumar, S. Mechanical and piezoresistive properties of GNP/UHMWPE composites and their cellular manufactured via selective laser sintering. *J. Mater. Res. Technol.* **2024**, *28*, 1359–1369. [[CrossRef](#)]
17. Zhu, L.; Pan, B.; Yang, Y.; Zhang, L.; Gao, H.; Tian, Z.; Wang, Y.; Du, S. Effects of marine environment on frictional properties of porous oil-impregnated  $\alpha$ -Al<sub>2</sub>O<sub>3</sub>/UHMWPE composites and molecular dynamics simulation. *Iran. Polym. J.* **2024**, 1–13. [[CrossRef](#)]
18. Kang, X.; Zhang, W.; Yang, C. Mechanical properties study of micro- and nano-hydroxyapatite reinforced ultrahigh molecular weight polyethylene composites. *J. Appl. Polym. Sci.* **2016**, *133*, 42869. [[CrossRef](#)]
19. ISO 527-1: 2019; Plastics—Determination of Tensile Properties—Part a: General Principles. International Organization for Standardization: Geneva, Switzerland, 2019.
20. ISO 604: 2002; Plastics—Determination of Compressive Properties. International Organization for Standardization: Geneva, Switzerland, 2002.
21. ISO 868: 2003; Plastics and Ebonite—Determination of Indentation Hardness by Means of a Durometer (Shore Hardness). International Organization for Standardization: Geneva, Switzerland, 2003.
22. Cheatwood, E.; Simon, G.; Crosby, L.; Goswami, T. Characterization of in vivo damage on retrieved total shoulder glenoid liners. *Lubricants* **2022**, *10*, 166. [[CrossRef](#)]
23. Ge, S.; Kang, X.; Zhao, Y. One-year biodegradation study of UHMWPE as artificial joint materials: Variation of chemical structure and effect on friction and wear behavior. *Wear* **2011**, *271*, 2354–2363. [[CrossRef](#)]
24. Qian, S. *Study on Friction Behavior About Natural Articular Cartilage*; China Univerairty of Mining and Technology: Xuzhou, China, 2009.
25. Gulmine, J.V.; Janissek, P.R.; Heise, H.M.; Akcelrud, L. Polyethylene characterization by FTIR. *Polym. Test* **2002**, *21*, 557–563. [[CrossRef](#)]
26. Azam, A.M.; Ali, A.; Khan, H.; Yasin, T.; Mehmood, M.S. Analysis of degradation in UHMWPE a comparative study among the various commercial and laboratory grades UHMWPE. *IOP Conf. Ser. Mater. Sci. Eng.* **2016**, *146*, 012025. [[CrossRef](#)]
27. Edidin, A.A.; Jewett, C.W.; Kalinowski, A.; Kwarteng, K.; Kurtz, S.M. Degradation of mechanical behavior in UHMWPE after natural and accelerated aging. *Biomaterials* **2000**, *21*, 1451–1460. [[CrossRef](#)] [[PubMed](#)]
28. Spece, H.; Yarbrough, R.V.; Kurtz, S.M. In vivo performance of vitamin E stabilized polyethylene implants for total hip arthroplasty: A review. *J. Arthroplast.* **2023**, *38*, 970–979. [[CrossRef](#)] [[PubMed](#)]
29. Hope, N.; Bellare, A. A comparison of the efficacy of various antioxidants on the oxidative stability of irradiated polyethylene. *Clin. Orthop. Relat. Res.* **2015**, *473*, 936–941. [[CrossRef](#)] [[PubMed](#)]
30. Narayan, V.S. Spectroscopic and chromatographic quantification of an antioxidant-stabilized ultrahigh-molecular-weight polyethylene. *Clin. Orthop. Relat. Res.* **2015**, *473*, 952–959. [[CrossRef](#)] [[PubMed](#)]
31. Wu, J.; Yang, T.; Dong, P.; Zhang, Q.; Wang, K. Simultaneously enhanced antioxidation and wear resistance in UHMWPE molded plastic by adding natural polyphenol antioxidant. *Polymer* **2024**, *304*, 127145. [[CrossRef](#)]
32. Borruto, A.; Crivellone, G.; Marani, F. Influence of surface wettability on friction and wear tests. *Wear* **1998**, *222*, 57–65. [[CrossRef](#)]
33. Belotti, L.P.; Vadivel, H.S.; Emami, N. Tribological performance of hygrothermally aged UHMWPE hybrid composites. *Tribol. Int.* **2019**, *138*, 150–156. [[CrossRef](#)]
34. Yin, Y.; Liu, F.; Miao, M.; Yuan, Z.; Tang, Y. Effect of surface roughness on the liquid bridge between two rigid spheres. *Powder Technol.* **2025**, *449*, 120377. [[CrossRef](#)]
35. Wu, G.; Chen, S.; Qin, H.; Zhao, C. Effect of wettability on tribological properties of porous UHMWPE. *Adv. Mater. Res.* **2012**, *549*, 670–673. [[CrossRef](#)]
36. Gürgen, S.; Çelik, O.N.; Kuşhan, M.C. Tribological behavior of UHMWPE matrix composites reinforced with PTFE particles and aramid fibers. *Compos. Part B Eng.* **2019**, *173*, 106949. [[CrossRef](#)]
37. Dusunceli, N.; Colak, O.U. Modelling effects of degree of crystallinity on mechanical behavior of semicrystalline polymers. *Int. J. Plast.* **2008**, *24*, 1224–1242. [[CrossRef](#)]
38. Wang, Y.J.; Wang, J.L. *Orthopaedic Biomechanics*; People's Military Medical Press: Beijing, China, 1989.
39. Li, F.; Zhou, H.; Su, Y.; Wang, C. Study on the compression properties between articular cartilage and polyvinyl alcohol hydrogel as artificial cartilage. *J. Med. Biomech.* **2009**, *24*, 448–451.
40. Burris, D.L.; Ramsey, L.; Graham, B.T.; Price, C.; Moore, A.C. How sliding and hydrodynamics contribute to articular cartilage fluid and lubrication recovery. *Tribol. Lett.* **2019**, *67*, 46. [[CrossRef](#)]

**Disclaimer/Publisher's Note:** The statements, opinions and data contained in all publications are solely those of the individual author(s) and contributor(s) and not of MDPI and/or the editor(s). MDPI and/or the editor(s) disclaim responsibility for any injury to people or property resulting from any ideas, methods, instructions or products referred to in the content.